Geometry-Material Coordination for Passive Adaptive Solar Morphing Envelopes

Sarah Mokhtar[1], Christopher Leung[1] and Angelos Chronis[2]

[1]University College London
London, United Kingdom
sarah.mokhtar.15@ucl.ac.uk, christopher.leung@ucl.ac.uk

[2]Intitute for Advanced Architecture of Catalonia
Barcelona, Spain
angelos.chronis@iaac.net

ABSTRACT

The cost-intensive and mechanical complexity natures of the adaptive facades of the past decades drifted designers and researchers' interest towards passive material-based actuation systems [5, 6, 10]. Architectural applications using the latter showed, however, a few limitations restricting the output possibility space to options that rely entirely on one material's phase characteristic. This study aims to investigate the potential of expanding a shape memory alloy-actuated facade's output from one that is limited and hardly controllable in the case of entirely passive actuation to one that can produce a specific desired performative target. This is explored through coordinating between geometry-movement connections of an adaptive component of four integrated shape memory alloys, which work on tailoring the geometry-material-climate relations of the responsive system. The research findings suggest that the integration of geometry, material, and their connections in the design of a SMA solar morphing envelope lead to the development of a wider range of behavioural system outputs. The variety instilled through these added dimensions promoted diversity and adaptability of output for a flexible range of responses and higher performative gains.

Author Keywords

Material Computation; Requisite Variety; Solar Morphing Envelopes; Smart Materials.

1 INTRODUCTION

The cost-intensive and mechanical complexity natures of the adaptive facades of the past decades drifted designers and researchers' interest towards passive material-based actuation systems [5, 6, 10]. Architectural applications using the latter showed, however, a few limitations restricting the output possibility space to options that rely entirely on one material's phase characteristic.

The Adaptive Skins and the Self-Adaptive Membrane projects [3, 12] constitute examples of applications utilizing solar radiation as the thermal trigger for shape memory alloy (SMA)[1]-actuation of their components. Each component was developed as an integration of several shape memory alloys (SMAs), and thus created wider geometrical possibilities through larger degrees of freedom on the components scale, overcoming the linearity of their material activation. These reflected the potentials of diversifying the material-based actuated components' outputs through careful design of the geometry-system relations.

The shift in the perception of materials' innate capabilities favour the understanding of this domain as computational, rather than mere situational convenience. A material can be recognized as an entity being at one state at any moment in time, the actual state; while having other available virtual states. Triggering the latter into actuality requires catalysts that can either be the manifestation of an essence or the force driving it into obtaining a certain form [2]. DeLanda explains that:

"a richer conception of causality linked to the notion of the structure of a possibility space gives us the means to start thinking about matter as possessing morphogenetic powers of its own".

An unveiling of these powers would thus require an understanding of the underlying system's production mechanism, and its possibility space's structure which includes its stable states and transitions between them [2]. By identifying the material system's rules and input variability, the resulting material's behaviour[2] can potentially be computed, predicted, or defined.

The material behaviour's complexity and the successful attempts in architectural applications suggest there are implications of material computation's concept for expanding the possibilities of its applicability through understanding, controlling and diversifying material triggers.

This study aims to investigate the potential of expanding a SMA-actuated facade component's output entirely passively from one that is limited to one that is capable of producing a specific desired performative target. This is explored through coordinating between geometry-movement connections of a 4-SMAs adaptive component, which works on tailoring geometry-material-climate relations of the adaptive system.

[1] SMAs are alloys that undergo lattice phase transformations, deforming in cold temperatures and recovering shape when heated [8].

[2] Considered as the computational system's output.

2 METHODOLOGY

To investigate the potentials of geometry-material-climate for a façade system actuated by shape memory alloys (SMAs), a case study context and its desired performative outputs are identified followed by a simplified SMA thermal model, pre-calculation of solar irradiation values for SMAs, and a coordination computational model used to carry out the study.

2.1 Case Study SMA Shading Structure

A generic 9 by 6 shading grid for a south-oriented façade in Cairo-Egypt climate is utilized using shape-memory actuated geometries of 400mm square panels [7]. Nine shading forms, shown in Figure 1, are considered, actuated using 4 shape memory alloys located on the four corners of the panel, illustrated in Figure 2. This system's design and performance evaluation (daylighting, solar incidence and openness) carried out in an in-depth previous study [7] was used to identify twenty desired performative configurations to test in this research. Each configuration consists of a façade combination of two of the nine shading forms, one for the upper portion of the façade grid and the other for the lower portion.

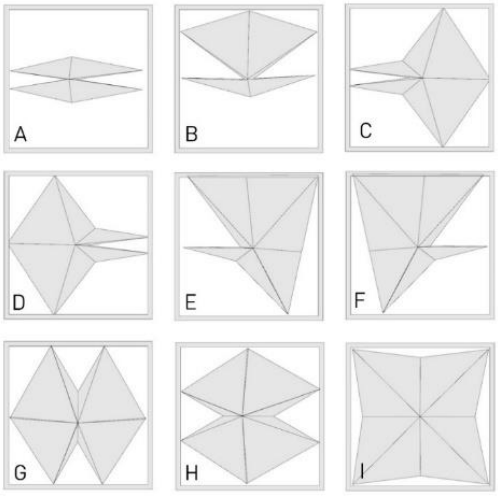

Figure 1. Nine Investigated Geometries [7]

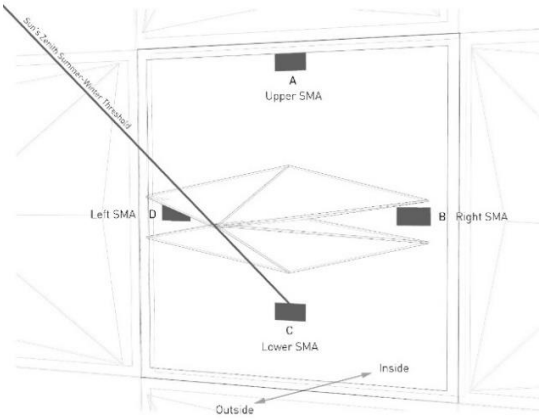

Figure 2. SMA Geometry Locations [7]

2.2 Simplified SMA Thermal Model

Modelling the SMA behaviour was necessary for the prediction of the actuation dynamics and material limitations. Due to the complexity and ambiguity in SMA behaviour models, a simplified approach was used for the estimation of the material temperature in the exterior environment. These calculations were performed for comparative objectives, contrasting different states under selective configurations, rather than for exact predictions.

According to the first law of thermodynamics, a system's total energy is conserved [4, p.13]. In general terms, under equilibrium conditions, the heat stored in the material can be defined as the thermal energy generated by an external source minus thermal losses due to conduction, convection and radiation as defined in Equation A from [11]:

$$\rho C V \frac{dT}{dt} = Q_e - Q_{conduction} - Q_{convection} - Q_{radiation} \quad \text{(A)}$$

where:

ρ	density of the SMA	in $kg \cdot m^{-3}$
C	specific heat capacity of the SMA	in $J \cdot kg^{-1} \cdot K^{-1}$
V	volume of the SMA	in m^3
T	temperature of the SMA at time t	in K
Q	thermal energy	in J

Q_e, where solar radiation is the source of external heat, the incident solar radiation on a material's surface is calculated; while the absorbed portion of that energy can be identified in correspondence with the material's capacity to absorb as described in Equation B from p.10 [4]:

$$Q_e = G_{abs} = \alpha s G = \varepsilon s G \quad \text{(B)}$$

where:

Q_e / G_{abs}	thermal energy absorbed by SMA	in W
α	absorptivity of the SMA	
s	surface area of the SMA	in m^2
G	solar irradiation	in $W \cdot m^{-2}$
ε	emissivity of the SMA, defined as equal to absorptivity in equilibrium	

For a large number of applications, $Q_{radiation}$ effect can be neglected, while $Q_{convection}$ can be expressed in Equation C from [11]:

$$Q_{convection} = hs(T - T_e) \quad \text{(C)}$$

where:

Q_{conv}	convective thermal energy loss	in W
h	heat-exchange coefficient between the SMA and medium	in $W \cdot m^{-2} \cdot K^{-1}$
T_e	temperature of the surrounding	in K

A common neglect of conduction for metallic alloys is justified by the assumption of temperature uniformity in the material because of its low internal heat conduction resistance. A 0.01 value for the Biot number is considered a

verification of the validity of that assumption, calculated with Equation D from [11].

$$B_i = \frac{hl}{k} \quad \text{(D)}$$

where:

B_i Biot number
l characteristic length, as wire diameter in m
k thermal conductivity of the SMA in $W \cdot m^{-1} \cdot K^{-1}$

The heat transfer SMA equation, modelling the SMA behaviour, can thus be simplified to Equation E as follows:

$$\rho C V \frac{dT}{dt} = \varepsilon s G - hs(T - T_e) \quad \text{(E)}$$

The heat exchange coefficient h, in convection, can be defined as function of the SMA thermal conductivity and characteristic length, defined as the wire volume per surface area as expressed in Equation F from [11]:

$$h = \frac{\lambda N_u}{l} \quad \text{(F)}$$

where:

λ thermal conductivity of the convective medium in $W \cdot m^{-1} \cdot K^{-1}$
N_u Nusselt number, defining the heat-exchange ratio in free convection

The Nusselt number, though, can be calculated using the characteristic Prandtl and Grashof numbers for the convective medium, air, were defined in Equation (G) from [11]:

$$N_U = \left(0.6 + \frac{0.387 (G_r P_r)^{\frac{1}{6}}}{\left[1 + (0.559/P_r)^{\frac{9}{16}}\right]^{\frac{8}{27}}} \right)^2 \quad \text{(G)}$$

where:

P_r Prandtl number for the convective medium
G_r Grashof number for the convective medium

Because of the phase change transformation and hysteresis of the SMA behaviour, the exact behaviour required further calculations of latent heat and adjustment of some temperature-dependent properties. Integrating the added stress from the component's weight would be necessary for an exact temperature, but was assumed here to be a light weight material hence negligible. Geometric properties were identified based on the required actuation length for the full geometry movement, suitable spring diameters and thicknesses. Due to the more common availability of SMA with various activation temperatures commercially produced and the possibility of their tailoring to the design needs, a range of temperatures were considered ranging from 20 to 100℃.

[3] Ladybug is an open source plugin that help evaluate and visualize environmental performance using imported data from EnergyPlus weather files [9]

Despite the wide variation in shape memory alloy types in terms of composition and transformation temperatures and their differentiated properties, thermal properties considered were values provided by a SMA material supplier for the most commonly used type, emissivity value estimated by experimental testing and air properties from similar SMA research [11, 13].

The following Table 1 identifies the geometric and physical properties of the SMA used for the approximate material behaviour modelling.

Table 1. Thermal and Physical SMA Characteristics and Convective Medium

Property	Value	Unit
SMA Thermal Properties		
Density ρ	6450	$kg \cdot m^{-3}$
Specific heat C	837	$J \cdot kg^{-1} \cdot K^{-1}$
Thermal conductivity k	18	$W \cdot m^{-1} \cdot K^{-1}$
Emissivity ε	0.82	-
Air Properties (20℃)		
Thermal conductivity λ	0.0257	$W \cdot m^{-1} \cdot K^{-1}$
Grashof number G_r	0.3903	-
Prandtl number P_r	0.713	-
Geometric and Calculated Properties		
Surface Area S	0.003142	m^2
Volume V	3.93×10^{-7}	m^3
Nusselt number N_u	0.739	-
Characteristic length l	5×10^{-4}	m
Heat-exchange coefficient h	38	$W \cdot m^{-2} \cdot K^{-1}$

2.3 SMAs Solar Irradiation Pre-Calculations

Per the thermal model examined in the previous section, the estimation of SMA temperature required two main input variables: the air temperature and the incident solar radiation on each SMA for a designated time and geometry. A representative time sample of the year was identified as hours ranging from 08:00 to 17:00 on the 21st of March, June, September and December, the equidoxes and solstices.

For each of the possible geometrical configurations, a solar irradiation analysis was carried out using Radiance engine through Ladybug[3] for the 40 selected hours of study, of which a sample is illustrated in Figure 3. The corresponding air temperature values were then extracted from Cairo EnergyPlus weather file. These radiation and air temperature values were pre-calculated and saved to reduce the necessary computational time for the coordination impacts investigations.

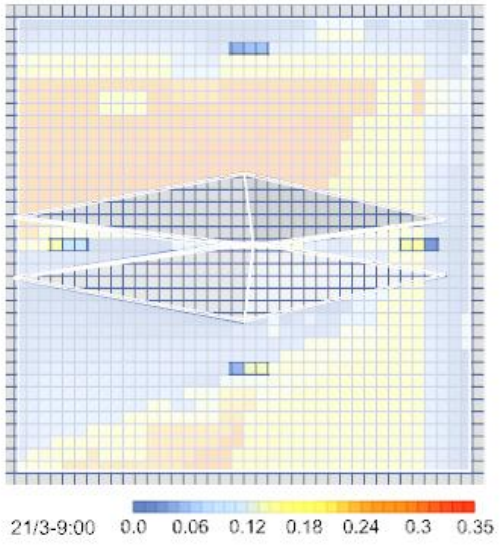

Figure 3. SMA Solar Irradiation Simulation

2.4 Coordination Computational Model

This section describes the methodology used to generate the SMA system characteristics necessary for the production of the desired adaptive output. These characteristics include the actuation temperatures of the four SMAs as well as their corresponding connections between actuators and movement. This approach regards the material system solution as an outcome of the interaction between the context, the performance, the material and the geometry, as illustrated in Figure 4.

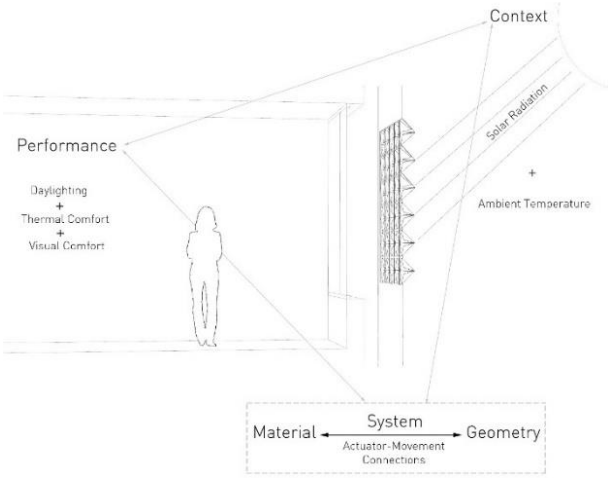

Figure 4. Context-Performance-Material-System-Geometry Interactions

All the connection configurations were identified, where one actuator can only be responsible for the deployment of one or two sides, shown below in Figure 5. The rationale behind excluding the combinations where one actuator can move three or four sides was that it reduced the variability highly desired in this research. This resulted in SMA systems consisting of two, three or four SMAs depending on performative need and behaviour. Finding the most conforming connection system and corresponding actuation temperatures required going through four phases.

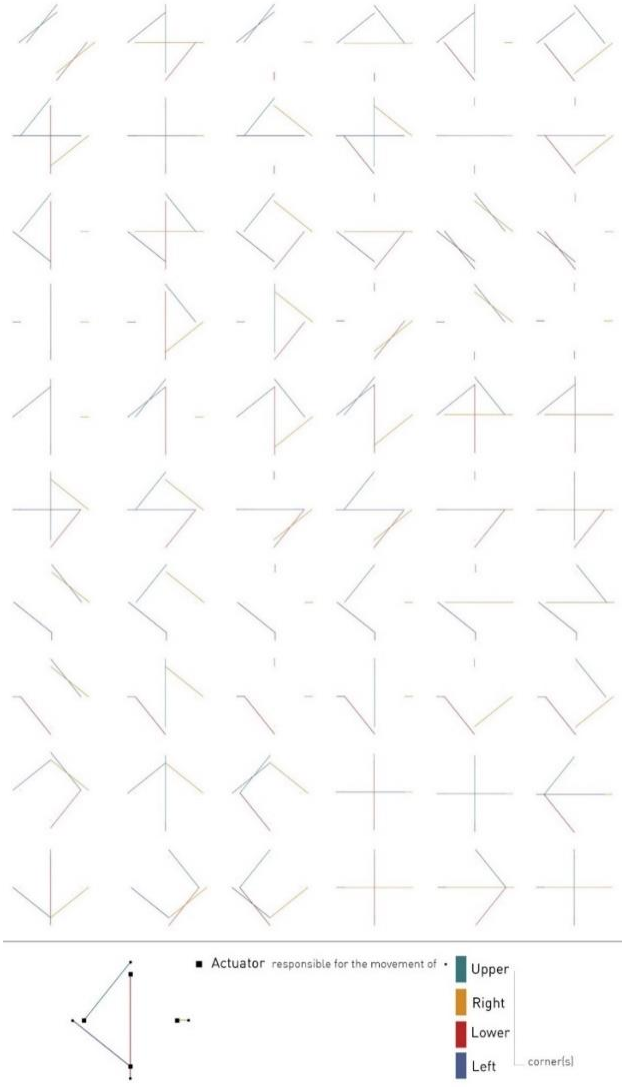

Figure 5. Actuator-Movement Connection Configurations

The first phase of actual SMA temperature calculations was based on the SMA thermal model discussed in the previous section. For the 40 hours studied (ranging from 08:00 to 17:00 on the 21st of March, June, September and December), the upper and lower portions of the façade were each characterized by one geometrical configuration. For each hour and for each geometry, a two-dimensional array indicated the 4-SMAs incident solar radiations represented in a 2x2 matrix in the following order: $\begin{bmatrix} Upper\ SMA & Eastern\ SMA \\ Lower\ SMA & Western\ SMA \end{bmatrix}$.

The calculations were carried out such that T_p in the equation was taken as the air temperature for 08:00 assuming minimal

radiation in earlier hours of day; while for all other hours, T_p corresponded to the SMA temperature at the previous state.

The second phase required, in addition to the SMA actual temperatures, two other sets of arrays for each geometry: the geometrical configurations (deployed side:1, undeployed:0), the actuator-connection alternatives, which indicated the actuator responsible for the corresponding movement (index:0-3). For each actuator-movement connection, for the sides connected to each actuator, a search was excecuted through the desired geometric configurations' list for the instances at which this side's geometry is deployed. For all the hours of deployed movements, the SMA temperatures of the corresponding actuator are aggregated in a list. The choice of the suitable temperature was then based on three alternative methods; the minimum, the most common and the average. This approach generated, for each connection type, a two dimensional array indicating the 4-SMAs suitable activation temperatures.

The generation of the resulting SMAs façade combinations, the third computational phase, used the defined 4-SMAs activation temperatures as the threshold to identify deployment status of each compoment 's side, and thus the geometrical configuration. These forms were then, in the fourth phase, compared to the original desired output matrix using four evaluation metrics: the compatiblity of the final geometries, the compatibility of the 4-SMA in deployment, the variety of possible forms within one day and within a year.

3 COORDINATION RESULTS

Large variations were observed between the ambient temperature and the four SMA temperatures over the year, as well as between each other for the same recorded hour. A range of difference expanding from 0 to 15 degrees Celcius was determined, with the largest variations reported in September and during radiation peak hours of winter. Figure 6 shows these variations for the most performing case as identified in the previous section.

Twenty of the highest performing cases were tested as desired output to generate most compatible SMA systems and identify their respective activation temperatures and connection types. Figure 7 and Figure 8 show the result of two samples, illustrated as a comparison between the desired geometrical states for each hour and the actual output achieved through the developed computational process. For each façade portion, a diagram was supplemented to identify the actuator-movement connections, the activation temperature of each SMA as well as an evaluation of their compatibility and diversity.

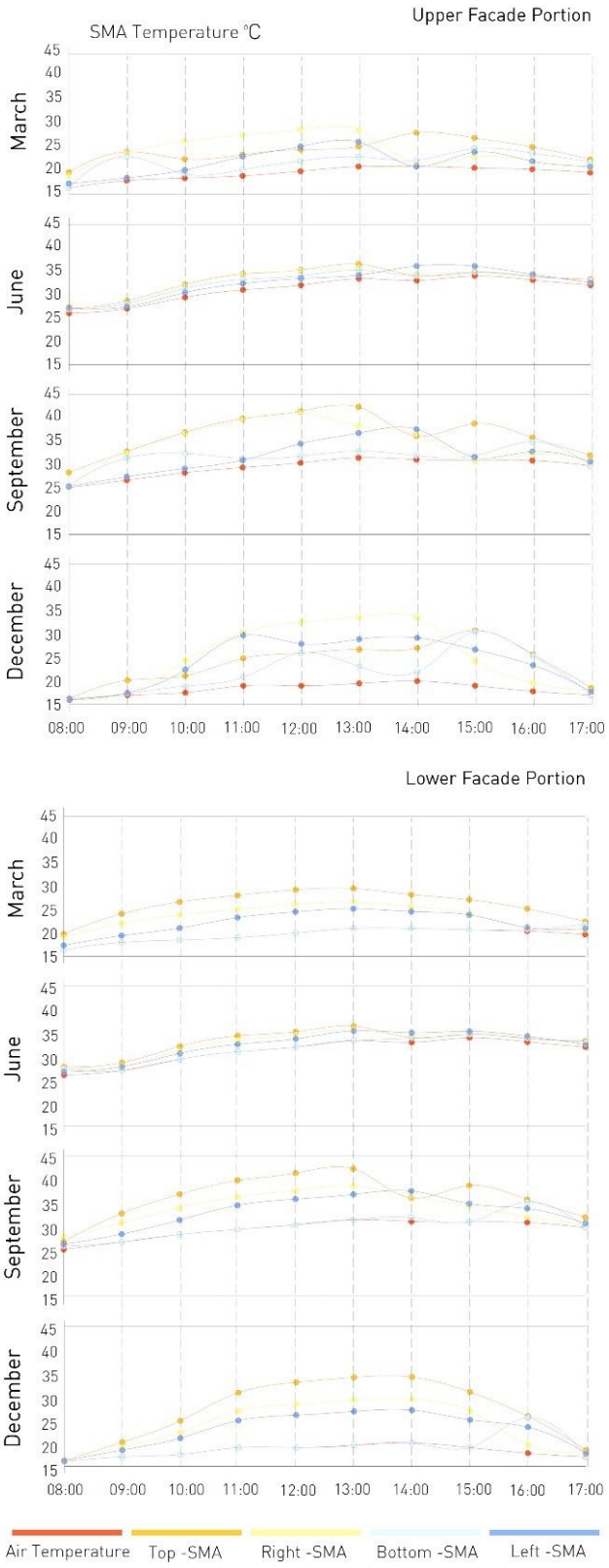

Figure 6. Variations between Ambient and 4-SMA Temperatures

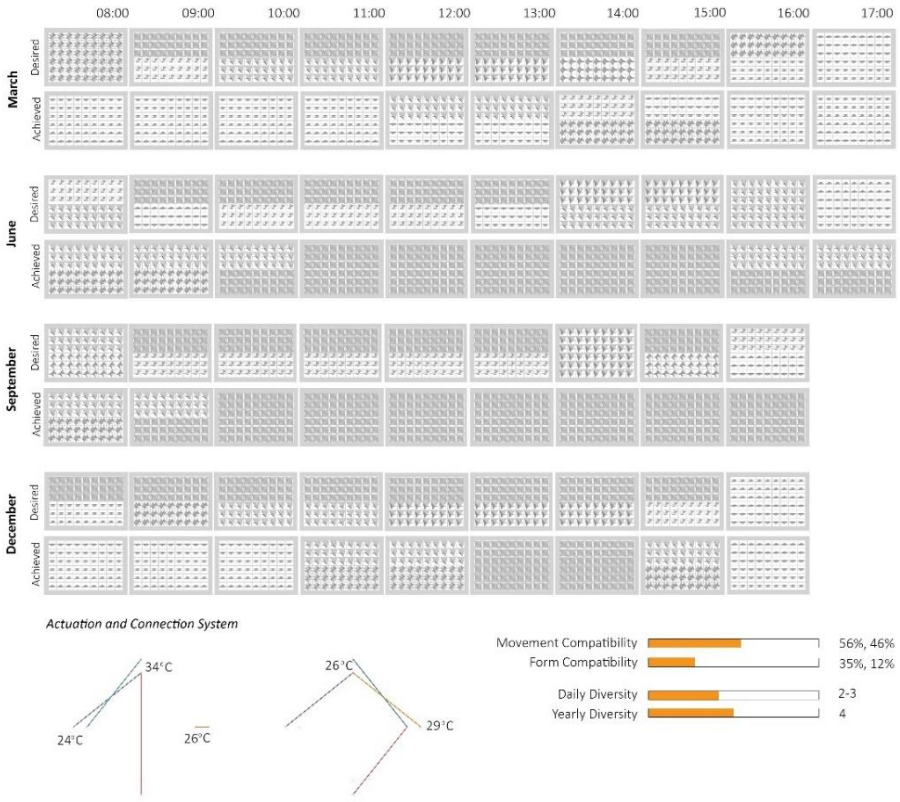

Figure 7. Sample Compatibility SMA Systems for Performative Case – A

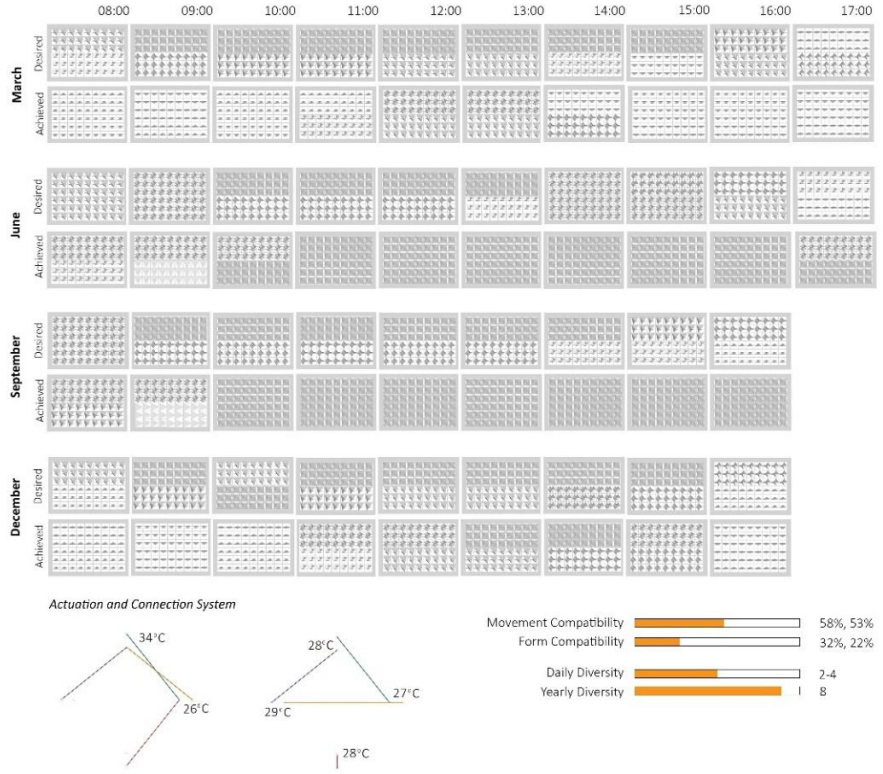

Figure 8. Sample Compatibility SMA System for Performative Case – B

4 DISCUSSION

The strategy used to engineer the SMA shading skin for the desired adaptability was developed to reach a tailored unique solution, a constraining restriction leading to maximum component and SMA compatibilities of 44% and 67% respectively. It is important to note that these calculations excluded all the cases which achieved higher compatability rates, up to 87%, but which only used the closed configuration in most hours. A more flexible targeted output would be more convenient for the façade's initial performative objective which achieves higher compatibility rates and daylighting values.

Additionally, high diversity rates were achieved for the cases with highest compatibility, reaching up to 4 different forms within one day and up to 6 during the year. The resulting behavioural diversity provided evidence for the design premise and the rise of a novel understanding of material-based shading systems as ones that can produce more than just binary outputs on the component's scale.

Partial results are illustrated below in Figure 9 showing the relation between actuator-movement connections and the evaluation criteria.

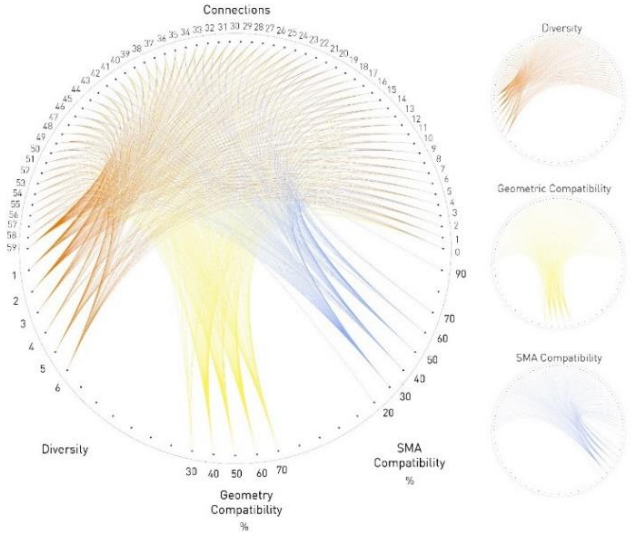

Figure 9. Actuator-Movement Connections Evaluated

The most conforming and diverse cases were identified by a characteristic range of temperature selection methods, activation temperatures and connections. The most common calculation strategy for the activation temperatures was through the identification of the most common within the list with an approximate 80%, followed by the average and none used the minimum method.

Activation temperatures, although calculated in the scope of this study for a comparative purpose, ranged between 18 and 37℃ which indicated the relevance of varying activation temperatures for higher ranges of acceptable systems. However, the highest performing system solutions showed a significant portion of varied connections with all actuators that have similar activation temperatures; demoting this differentiation potential to an important but secondary level of impact.

Connection differentiations between actuators and movements provided insights into the possibilities that this approach unveiled and the degree of adaptability improvement it added. The standard connection, with each actuator connected to the closest movement, was rarely successful; showing the higher resulting ranges achievable by allowing actuators to be responsible for one or two non-direct movements. Despite the variation relevance, about 40% of the connections did not show in the best compatability results, which reflects that some may be eliminated from the search with no major impact on the solution performance.

The solar radiation simulation along with the computational model methodologies provided the means to carry out this research; however carried several constraints. These mainly include their entire dependence on the accuracy of the digital simulations of Cairo's weather file and on the negligable impact of climatic factors other than temperature and radiation such as humidity, wind and others.

The complexity, inaccuracy and experimental base of the developed SMA thermal models in the literature [8] as well as the need for comparative rather than accurate behavioural predictions for this particular study provided a grounded rationale for the use of a significantly simplified model of the actual SMA behaviour. The inaccuracies in material temperature estimations were mainly affected by the determined values for emissivity and convective heat transfer, the assumption of their constant values during the martensitic and austenitic phases and the hysteresis effect. An estimate of 0.82 emissivity was used constantly, while the literature has shown a 9% emissivity variation between martensitic and austenitic states [1]. Determining the SMA convective heat transfer coefficient was the subject of many attempts in material science research and the predicted values varied significantly. The Velazquez and Pissaloux's model was used to determine the convective heat transfer coefficient used in this study's thermal model as a function of the Nusselt number under 20℃ free air, SMA thermal conductivity and characteristic length, reaching a value of 38 $W \cdot m^{-2} \cdot K^{-1}$. The implication of such a wide range of error for this estimation gave rise to the problematic arena of modelling SMA exact behaviour. However, since the study's objective was comparative and based on large time intervals, the simplified thermal model used was found adequate for this specific objective although better predictions could have been made by incorporating physical measurements and more developed thermal models.

The flexibility and adaptability present because of tailoring possibilities of phase temperatures and engineering properties based on composition, had an important impact on

the SMA's system computability capacities. If restricted to only one or two different temperatures, the resulting compatibility rates that this study showed would have been significantly lower.

5 CONCLUSION

The study showed that the integration of geometry, material, and their connections in the design of a SMA solar morphing envelope lead to the development of a wider range of behavioural system outputs. The variety instilled through these added dimensions promoted diversity and adaptability of output with a flexible range of desired responses. Despite the site-specific nature of this research, its findings are transferrable to similar hot dry climates with minimal sky coverage and comparable seasonal and hourly variations, and its study methodology is applicable to any context.

The positive impact of connection variations in achieving diversity provided insight into their computational potential which can be augmented through further studies into designing them as series of inputs capable of producing logical operations through either mechanical or sequential linkages. Research into material capacities for such architectural applications as well as experimental testing of real scale devices in targeted climates would allow for the development of a tailored and verified thermal model for SMA behaviour under targeted conditions. The latter will allow for better behavioural predictions thus higher conformance with performance objectives and provide insights into limitations of transferring this design approach to a constructible working material system.

REFERENCES

1. Costa Sa, M., Da Silva, E., Da Silva, F., Da Silva, T.: Emissivity Measurements on Shape Memory Alloys. Presented at the 2016 Quantitative InfraRed Thermography, January (2016)
2. DeLanda, M.: The New Materiality, (2015)
3. Gonzalez, N., More, S.: Self-Adaptive Membrane: Kinetic Passive System. Institute for Advanced Architecture of Catalonia (2015)
4. Incropera, F., Lavine, A., Bergman, T., DeWitt, D.: Fundamentals of Heat and Mass Transfer. John Wiley & Sons (2011)
5. Kolarevic, B.: Actualising (Overlooked) Material Capacities, (2015)
6. Kolarevic, B., Parlac, V.: Adaptive, Responsive Building Skins. In: Building Dynamics: Exploring Architecture of Change. pp. 69–88. Routledge (2015)
7. Mokhtar, S.: Material-Based Actuation of Facades: An Adaptive Performative Approach. University College London (2016)
8. Otsuka, K., Wayman, C.: Shape Memory Materials. Cambridge (1998)
9. Roudsari, M., Pak, M.: Ladybug: A Parametric Environmental Plugin for Grasshopper to Help Designers Create an Environmentally-Conscious Design. In: Proceedings of BS2013. pp. 3128–3135. , France (2013)
10. Speck, T., Knippers, J., Speck, O.: Self-X Materials and Structures in Nature and Technology, (2015)
11. Velazquez, R., Pissaloux, E.: Modelling and Temperature Control of Shape Memory Alloys with Fast Electrical Heating. Int. J. Mech. Control. 13 (2), 1–8 (2012)
12. Verma, S., Devadass, P.: Adaptive Skins: Responsive Building Skin Systems based on Tensegrity Principles. AA School of Architecture (2013)
13. Technical Characteristics of Flexinol Actuator Wires. Dynalloy Inc., California